PHILOSOPHICAL TRANSACTIONS OF THE ROYAL SOCIETY A MATHEMATICAL, PHYSICAL & ENGINEERING SCIENCES

Three–dimensional boundary–layer flow past a cusp secured to a flat plate

G. G. Vilensky

Phil. Trans. R. Soc. Lond. A 2000 **358**, 3155-3167
doi: 10.1098/rsta.2000.0702

10.1098/rsta.2000.0702

THE ROYAL SOCIETY

Three-dimensional boundary-layer flow past a cusp secured to a flat plate

By G. G. Vilensky

Research and Production Enterprise Marine Equipment 46, Primorsky Prospect, St Petersburg 197374, Russia

The paper deals with the boundary-layer flow developing near the rib of the corner formed by a flat plate and a cusp secured to its surface. The analysis focuses on the asymptotic description of the plate's flow. The latter is shown to consist of two characteristic domains, each containing its own boundary layer. One of them develops from the leading edge of the plate, whereas the other one starts from the rib of the corner. The work concentrates on the mechanism of flow adjustment in the region where these two boundary layers overlap.

Keywords: boundary layer; viscous flow; marched asymptotic expansions; flow collisions

1. Introduction

Owing to their practical importance, three-dimensional viscous flows in corner regions have been studied extensively experimentally, numerically and theoretically. Some impression of the state of the art can be derived from the publications by Rubin (1966), Anderson *et al.* (1990), Smith & Gajjar (1984), Walton & Smith (1997) and Dhanak & Duck (1997). A detailed analysis of literature on this issue is presented in Dhanak & Duck (1997). In the theoretical sense, such flows present a model that permits one to gain an insight into the structure of an essentially three-dimensional viscous flow. The purpose of the present work is to study the particular flow case when the walls of the corner are curved so as to exert a large cross-stream pressure gradient on the secondary viscous motion. The paper deals with the flow about a streamlined corner formed by a cusp and a flat plate, as shown in figure 1. The details of the geometry and the related potential flow solution are outlined in § 2. In § 3 we show that this flow configuration is remarkable for the simultaneous existence of two boundary-layer flows at the surface of the plate. One of them develops from the leading edge of the plate, as would normally be expected, whereas the other one originates from the rib of the corner OL and is driven by the favourable cross-stream pressure gradient created by the cusp. Both flows merge in a buffer region. Its characteristic feature is the coexistence of the two opposite directions of disturbance propagation, each one associated with the related incoming boundary-layer flow. This makes the buffer region inaccessible for the usual numerical marching procedures. However, it appears that consistent flow description is still possible within the framework of the conventional boundary-layer approach without recourse to full equations of motion.

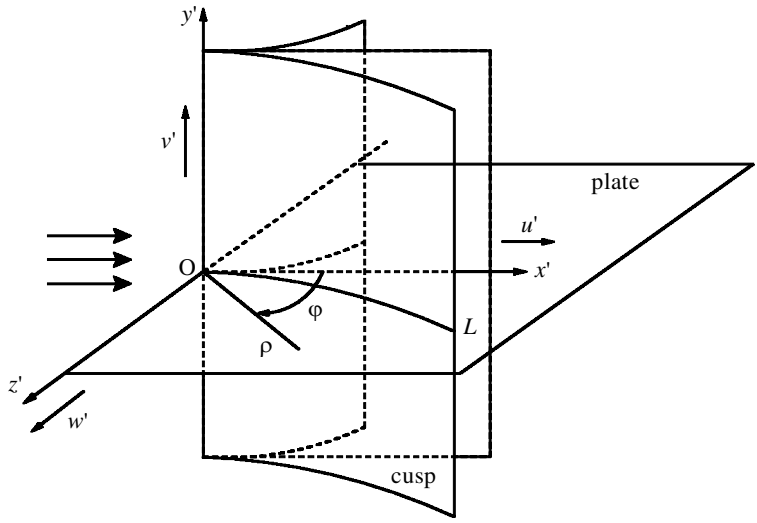

Figure 1. Flow geometry.

2. Potential flow

Consider an incompressible inviscid flow past a three-dimensional corner formed by a semi-infinite flat plate and a streamlined cusp secured vertically to the plate's surface so that the leading edges of the cusp and the plate intersect at a right angle at a point O, as in figure 1. Introduce a Cartesian frame $l(\mathrm{O}, x', y', z')$. The axes $\mathrm{O}y'$ and $\mathrm{O}z'$ coincide with the leading edge of the cusp and the plate, respectively. The axis $\mathrm{O}x'$ is normal to the plane $\mathrm{O}y'z'$. The plate satisfies the relations $y' = 0$, $x' \geqslant 0$. The walls of the cusp near the origin are given by the equation $z' = \pm b(x')^{\alpha}/\alpha + \cdots$, as $x' \to 0$; b is a positive constant, $\alpha > 1$. The projections of the velocity vector on the coordinates $l(x', y', z')$ are $U_{\infty}(u', v', w')$. The non-dimensional pressure is $p' = (p - p_{\infty})/(\rho_* U_{\infty}^2)$. Here p is the pressure at a given point, $\rho_* = \text{const.}$ is the fluid density, p_{∞} and U_{∞} are the pressure and the velocity in the incident freestream, which is uniform and parallel to the x'-axis. l is a characteristic length-scale.

Let us first consider the inviscid flow outside any boundary layer. Assume that the motion is irrotational and introduce the flow potential Φ: $\nabla\Phi = (u', v', w')$. It satisfies Laplace's equation in the fluid domain,

$$\left(\frac{\partial^2}{\partial x'^2} + \frac{\partial^2}{\partial y'^2} + \frac{\partial^2}{\partial z'^2}\right)\Phi = 0, \tag{2.1}$$

and the boundary conditions of zero normal velocity on the cusp and the plate, respectively:

$$\frac{1}{\sqrt{1 + b^2 (x')^{2\alpha-2}}}\left(\mp b(x')^{\alpha-1}\frac{\partial\Phi}{\partial x'} + \frac{\partial\Phi}{\partial z'}\right) = 0 \quad \text{on } z'|_{x\to 0} = \pm b(x')^{\alpha}/\alpha + \cdots, \tag{2.2}$$

$$\frac{\partial\Phi}{\partial y'} = 0 \quad \text{on } y' = 0, \quad x' \geqslant 0. \tag{2.3}$$

In order to obtain a physically realistic solution, we require that the velocity be finite:

$$|\nabla\Phi| < \infty \quad \text{as } r \equiv \sqrt{x'^2 + y'^2 + z'^2} \to 0. \tag{2.4}$$

In what follows, we shall confine the analysis to the study of the local flow in the vicinity of the point O, where $r \to 0$. Thus, no boundary conditions at infinity are imposed here.

Since the width of the cusp near its leading edge is $O((x')^\alpha)$, the cusp surface is described by $z' = 0$ to leading order, and the boundary condition (2.2) reduces to (2.2′):

$$\frac{\partial\Phi}{\partial z'} = 0 \quad \text{on } z' = 0. \tag{2.2′}$$

The problem (2.1), (2.2′), (2.3), (2.4) possesses the following set of eigenfunctions:

$$r^{2j+\gamma} C_{2j}^{\gamma+1/2}(\cos\vartheta)(\sin\vartheta)^\gamma \cos(\gamma\varphi), \quad \gamma = k/2, \quad k = 0, 1, 2, 3, \ldots, \quad j = 0, 1, 2, 3, \ldots.$$

Here,

$$y' = r\cos\vartheta, \quad x' = r\sin\vartheta\cos\varphi, \quad z' = r\sin\vartheta\sin\varphi, \quad 0 \leqslant \varphi \leqslant 2\pi, \quad 0 \leqslant \vartheta \leqslant \pi, \quad C_{2j}^{\gamma+1/2}(s)$$

are ultraspherical polynomials as defined in Abramovitz & Stegun (1979). Following Nazarov & Plamenevskij (1991), we construct the asymptotic solution (as $r \to 0$) to the problem (2.1)–(2.4) in the form of the series in these eigenfunctions and the forced terms resulting from the above reduction of the boundary condition (2.2) to the plane $z' = 0$. It will suffice, for our purposes, to consider only the main terms of the solution:

$$\Phi = \text{const.} + U_0 x' + \underline{U_0 b \alpha^{-1} \rho^\alpha \left(\frac{1 + \cos 2\pi\alpha}{\sin 2\pi\alpha} \cos\alpha\varphi + \sin\alpha\varphi \right)} + \{\text{forced terms if } \alpha < 5/4\} + c_1 \rho^{3/2} \cos\tfrac{3}{2}\varphi + \cdots, \quad \text{if } 1 < \alpha < \tfrac{3}{2}. \tag{2.5 a}$$

Here, $\rho = \sqrt{x'^2 + z'^2} \ll 1$, U_0 is the velocity at the point O, and c_1 is an arbitrary constant that depends on the global flow structure. The first, second and last terms in (2.5 *a*) are the local eigenfunctions.

When $\alpha = \frac{3}{2}$ the order of magnitude of the underlined forced term coincides with that of the eigenfunction $\rho^{3/2}\cos\frac{3}{2}\varphi$, and the sought solution takes the following form:

$$\Phi = \text{const.} + U_0 x' + \rho^{3/2}(c_1 \cos\tfrac{3}{2}\varphi + \tfrac{2}{3} U_0 b \sin\tfrac{3}{2}\varphi) + \cdots, \quad \text{if } \alpha = \tfrac{3}{2}. \tag{2.5 b}$$

When $\alpha > \frac{3}{2}$ the local solution is dominated by the above mentioned three eigenfunctions. Thus, without loss of generality in what follows we shall assume that

$1 < \alpha \leqslant \frac{3}{2}$. For the velocity vector and the pressure we have ($1 < \alpha < \frac{3}{2}$)

$$u' = U_0 + U_0 b \rho^{\alpha-1}\left[\frac{1+\cos 2\pi\alpha}{\sin 2\pi\alpha}\cos((\alpha-1)\varphi) + \sin((\alpha-1)\varphi)\right] + \cdots, \tag{2.6 a}$$

$$v' = \text{const.}\left(2r\cos\vartheta {C_2}^{1/2}(\cos\vartheta) - \rho\sin\vartheta\frac{\mathrm{d}C_2^{1/2}(\cos\vartheta)}{\mathrm{d}\cos\vartheta}\right) + \cdots, \tag{2.6 b}$$

$$w' = U_0 b \rho^{\alpha-1}\left[-\frac{1+\cos 2\pi\alpha}{\sin 2\pi\alpha}\sin((\alpha-1)\varphi) + \cos((\alpha-1)\varphi)\right] + \cdots, \tag{2.6 c}$$

$$p' = p_0 - U_0^2 b \rho^{\alpha-1}\left[\frac{1+\cos 2\pi\alpha}{\sin 2\pi\alpha}\cos((\alpha-1)\varphi) + \sin((\alpha-1)\varphi)\right] + \cdots, \tag{2.6 d}$$

where $p_0 = p'(0,0,0)$. Here and everywhere below the solution for $\alpha = \frac{3}{2}$ can be obtained from the solution for the case $\alpha < \frac{3}{2}$ (i.e. from (2.6) in the present context) by formal substitution of c_1 for $U_0 b(1+\cos 2\pi\alpha)/\sin 2\pi\alpha$.

Finally, note that when $\alpha = \frac{3}{2}$ and $c_1 = 0$ the pressure is constant along the surfaces $\varphi = 0, 2\pi$. Hence, with an appropriate choice of the higher-order terms the walls of the cusp, $z' = \pm b(x')^\alpha/\alpha + \cdots$, become free streamsurfaces. In this case, the obtained solution coincides locally with the two-dimensional results of Kirchhoff free streamline theory (see Imai 1953; Sychev *et al.* 1987), i.e.

$$u' = U_0 + U_0 b \rho^{1/2}\sin\varphi/2 - \tfrac{5}{6}U_0^2 b^2 x' + \cdots,$$
$$w' = U_0 b \rho^{1/2}\cos\varphi/2 + \tfrac{5}{6}U_0^2 b^2 z' + \cdots,$$
$$p' = p_0 - U_0 b \rho^{1/2}\sin(\varphi/2) - \tfrac{1}{2}(U_0^2 b^2 \rho) + \tfrac{5}{6}U_0^2 b^2 x' - \tfrac{5}{6}U_0^2 b^2 z' + \cdots.$$

3. Boundary-layer flow at the plate

Consider three-dimensional boundary-layer flow along the plate $y' = 0$ which develops from its leading edge $x' = y' = 0$ (see figure 1). Assume that the global Reynolds number $Re = LU_\infty/\nu$ is large (ν is the kinematic viscosity of the fluid), so that the flow is governed by the equations

$$u'\frac{\partial u'}{\partial x'} + v_Y\frac{\partial u'}{\partial Y} + w'\frac{\partial u'}{\partial z'} = -\frac{\partial p'}{\partial x'} + \frac{\partial^2 u'}{\partial Y^2}, \tag{3.1 a}$$

$$u'\frac{\partial w'}{\partial x'} + v_Y\frac{\partial w'}{\partial Y} + w'\frac{\partial w'}{\partial z'} = -\frac{\partial p'}{\partial z'} + \frac{\partial^2 w'}{\partial Y^2}, \tag{3.1 b}$$

$$\frac{\partial p'}{\partial Y} = 0, \tag{3.1 c}$$

$$\frac{\partial u'}{\partial x'} + \frac{\partial v_Y}{\partial Y} + \frac{\partial w'}{\partial z'} = 0, \tag{3.1 d}$$

subject to no-slip and main-stream conditions

$$u' = v_Y = w' = 0 \quad \text{on } Y = 0, \tag{3.2 a}$$

$$u' \to U_0, \quad \text{as } Y \to \infty, \tag{3.2 b}$$

$$w' \to U_0 b \rho^{\alpha-1}\left[-\frac{1+\cos 2\pi\alpha}{\sin 2\pi\alpha}\sin((\alpha-1)\varphi) + \cos((\alpha-1)\varphi)\right], \quad \text{as } Y \to \infty. \tag{3.2 c}$$

Here, $v_Y = Re^{1/2}v'$ and $Y = Re^{1/2}y'$, $1 < \alpha \leqslant \frac{3}{2}$. The pressure gradient on the right-hand side of (3.1 *a*), (3.1 *b*) is determined by the expression (2.6 *d*). In line with the note made at the end of § 2, the first term in (3.2 *c*) should be omitted when the cusp is formed by the free surface.

(*a*) *Main part of the boundary layer*

Consider the main part of the plate's boundary layer, where $\varphi = O(1)$. We take $x = x'$, $\varphi = \arctan z'/x'$, $\tilde{\eta} = Y/\sqrt{x'}$ for new independent variables instead of (x', Y, z'). In this notation, the boundary-layer flow stems from the leading edge of the plate $\varphi = \pi/2$ (or $\varphi = 3\pi/2$) and develops towards $\varphi = 0$ (or $\varphi = 2\pi$, respectively), which corresponds to the plane $Ox'y'$ (see figure 1). For definiteness in what follows we shall consider the interval $0 \leqslant \varphi \leqslant \pi/2$.

The solution to the system (3.1)–(3.2) is sought in the form ($\rho \to 0$):

$$u' = \frac{\partial \tilde{f}(\tilde{\eta}, \varphi)}{\partial \tilde{\eta}} + \cdots, \quad w' = \rho^{\alpha-1} w(\tilde{\eta}, \varphi) + \cdots, \quad v_Y = \frac{1}{\sqrt{x}} v(\tilde{\eta}, \varphi) + \cdots. \tag{3.3}$$

Substitution into equations (3.1)–(3.2) gives

$$\frac{\partial^3 \tilde{f}}{\partial \tilde{\eta}^3} + \tfrac{1}{2}\tilde{f}\frac{\partial^2 \tilde{f}}{\partial \tilde{\eta}^2} + \tfrac{1}{2}\sin 2\varphi \left(\frac{\partial \tilde{f}}{\partial \tilde{\eta}} \frac{\partial^2 \tilde{f}}{\partial \varphi \partial \tilde{\eta}} - \frac{\partial^2 \tilde{f}}{\partial \tilde{\eta}^2} \frac{\partial \tilde{f}}{\partial \varphi} \right) = 0,$$

$$\tilde{f} = \frac{\partial \tilde{f}}{\partial \tilde{\eta}}\bigg|_{\tilde{\eta}=0} = 0, \quad \frac{\partial \tilde{f}}{\partial \tilde{\eta}}\bigg|_{\tilde{\eta}=\infty} = U_0, \tag{3.4}$$

$$\frac{\partial^2 w}{\partial \tilde{\eta}^2} + \tfrac{1}{2}\tilde{f}\frac{\partial w}{\partial \tilde{\eta}} - (\alpha - 1)\cos^2\varphi \frac{\partial \tilde{f}}{\partial \tilde{\eta}} w + \tfrac{1}{2}\sin 2\varphi \left(\frac{\partial \tilde{f}}{\partial \tilde{\eta}} \frac{\partial w}{\partial \varphi} - \frac{\partial w}{\partial \tilde{\eta}} \frac{\partial \tilde{f}}{\partial \varphi} \right)$$
$$+ U_0^2 b(\alpha - 1)\cos\varphi \left[-\frac{1 + \cos 2\pi\alpha}{\sin 2\pi\alpha} \sin((\alpha - 2)\varphi) + \cos((\alpha - 2)\varphi) \right] = 0, \tag{3.5 a}$$

$$w|_{\tilde{\eta}=0} = 0, \quad w|_{\tilde{\eta}=\infty} = U_0 b \left[-\frac{1 + \cos 2\pi\alpha}{\sin 2\pi\alpha} \sin((\alpha - 1)\varphi) + \cos((\alpha - 1)\varphi) \right]. \tag{3.5 b}$$

Also,

$$v = \frac{1}{2}\left(\tilde{\eta}\frac{\partial \tilde{f}}{\partial \tilde{\eta}} - \tilde{f} \right) + \cos\varphi \sin\varphi \frac{\partial \tilde{f}}{\partial \varphi}.$$

Appropriate initial conditions can be obtained by setting $\varphi = \pi/2$ in (3.4), (3.5), in which case the problem reduces to the two-dimensional Blasius solution for a flat plate.

It may be observed from (3.4) that the streamwise pressure gradient does not affect the main-order equation for the longitudinal velocity component u'. This is due to the fact that this study is focused on the vicinity of the point O, which is close to the plate's leading edge. Thus, inertial and viscous forces in the emerging boundary layer are estimated as $u'\partial u'/\partial x' \sim (x')^{-1}$ and $\partial^2 u'/\partial Y^2 \sim (x')^{-1}$, i.e. are $O(\rho^{-1})$, whereas the pressure gradient is only $O(\rho^{\alpha-2})$, as can be seen from (2.6 *d*). However, the

crosswise pressure gradient appears in the cross-stream momentum equation (3.5 *a*). Since the crosswise velocity w' is much smaller than u', this equation is linear.

The system (3.4) yields the Blasius solution for the function $\tilde{f}$. Equations (3.5) can be integrated numerically in the usual fashion. The obtained solution is regular for all α. The skin friction $\partial w/\partial\tilde{\eta}(\tilde{\eta}=0,\varphi)$ grows from its Blasius value at the leading edge, $\varphi=\pi/2$, to a fixed value at $\varphi=0$. In the limit $\varphi=0$, equations (3.5) reduce to the following problem

$$w_{\tilde{\eta}\tilde{\eta}}+\tfrac{1}{2}\tilde{f}w_{\tilde{\eta}}-(\alpha-1)\tilde{f}_{\tilde{\eta}}w+{U_0}^2b(\alpha-1)=0,\quad w(0)=0,\quad w(\infty)=U_0b. \tag{3.6}$$

Here, the subscript $\tilde{\eta}$ stands for the corresponding derivative. For $\alpha=1.0$, 1.1, 1.2, 1.3, 1.4, 1.5, numerical integration of (3.6) gives the following values of the skin friction coefficient: $w_{\tilde{\eta}}(0)=0.33$, 0.47, 0.59, 0.71, 0.82, 0.92 ($U_0=b=1$).

Limiting streamlines are governed by the equation

$$\frac{\mathrm{d}z'}{\mathrm{d}x'}=\rho^{\alpha-1}\frac{\partial w(\tilde{\eta},\varphi)/\partial\tilde{\eta}}{\partial^2\tilde{f}(\tilde{\eta},\varphi)/\partial\tilde{\eta}^2}\bigg|_{\tilde{\eta}=0}+\cdots,\quad \rho\to 0. \tag{3.7}$$

Its numerical integration shows that limiting streamlines that stem from the leading edge of the plate at first develop towards the cusp. However, under the growing influence of the crosswise pressure gradient, they are gradually deflected from the cusp and do not reach its surface. Instead, there arises a particular limiting streamline

$$z'=\frac{(x')^\alpha}{\alpha}\frac{\partial w/\partial\tilde{\eta}}{\partial^2\tilde{f}/\partial\tilde{\eta}^2}\bigg|_{\tilde{\eta}=\varphi=0}+\cdots,\quad x'\to 0, \tag{3.8}$$

which bounds the rest of the above limiting streamlines from the cusp. Thus, the gap between the limiting streamline (3.8) and the cusp surface, $z'=b(x')^\alpha/\alpha+\cdots$, is inaccessible for the near-wall layer of the viscous flow developing from the leading edge of the plate.

Formal numerical integration of (3.7) shows that this gap is filled by another set of limiting streamlines. They stem from the cusp and develop to the line (3.8). However, this set of limiting streamlines must be discarded as physically unrealistic. The reason for this is that the obtained solution to the systems (3.4) and (3.5), which we use to integrate equation (3.7), is based on the initial conditions at the leading edge of the plate. As we have just seen in the previous paragraph, this solution cannot be continued into the immediate vicinity of the cusp surface; thus, it is inapplicable there.

It may also be observed that along the full vertical extent of the boundary layer, the velocity component normal to the cusp surface,

$$\frac{-b(x')^{\alpha-1}u'(\tilde{\eta},\varphi)+\rho^{\alpha-1}w(\tilde{\eta},\varphi)}{\sqrt{1+b^2(x')^{2\alpha-2}}}\approx(x')^{\alpha-1}(-bu'(\tilde{\eta},0)+w(\tilde{\eta},0)),$$

is non-zero on the cusp $z'=b(x')^\alpha/\alpha+\cdots$. (The exceptions are the plate $\tilde{\eta}=0$ and the outer boundary $\tilde{\eta}=\infty$.) This suggests that an additional sublayer must be set up near the cusp, in order to satisfy the condition of zero normal velocity on the cusp surface.

(*b*) *Nonlinear sublayer near the cusp wall*

It is reasonable to demand that the scale of this sublayer be compatible with the thickness of the cusp in the leading-edge region, i.e. $O((x')^{\alpha})$. So, let us introduce new crosswise scaling $\tau = (z' - b(x')^{\alpha}/\alpha)/(b(x')^{\alpha})$. (We note in passing that this scaling can be also derived from the equation of the accessibility line (3.8).) The solution (3.3) suggests the following expansions:

$$u' = \frac{\partial \bar{f}}{\partial \tilde{\eta}} + \cdots, \quad w' = b(x')^{\alpha-1}\left[\frac{\partial \bar{f}}{\partial \tilde{\eta}} + \frac{\partial \bar{g}}{\partial \tilde{\eta}}\right] + \cdots, \quad v_Y = \frac{1}{\sqrt{x'}}\bar{v}(\tilde{\eta}, \tau) + \cdots. \tag{3.9}$$

Here, $x' \to 0$, while $\tilde{\eta}$ and τ are $O(1)$; $\bar{f}(\tilde{\eta}, \tau)$ and $\bar{g}(\tilde{\eta}, \tau)$ are unknown functions. Notice that $b(x')^{\alpha-1}\partial\bar{g}/\partial\tilde{\eta}$ is the main term of the expansion of the velocity component normal to the cusp surface. Substitution of (3.9) into (3.1), (3.2) leads to the following nonlinear system:

$$\frac{\partial^3 \bar{f}}{\partial \tilde{\eta}^3} + \tfrac{1}{2}\bar{f}\frac{\partial^2 \bar{f}}{\partial \tilde{\eta}^2} + \left(\alpha\tau\frac{\partial \bar{f}}{\partial \tilde{\eta}} - \frac{\partial \bar{g}}{\partial \tilde{\eta}}\right)\frac{\partial^2 \bar{f}}{\partial \tau \partial \tilde{\eta}} - \left(\alpha\tau\frac{\partial \bar{f}}{\partial \tau} - \frac{\partial \bar{g}}{\partial \tau}\right)\frac{\partial^2 \bar{f}}{\partial \tilde{\eta}^2} = 0, \tag{3.10 a}$$

$$\frac{\partial^3 \bar{g}}{\partial \tilde{\eta}^3} + \tfrac{1}{2}\bar{f}\frac{\partial^2 \bar{g}}{\partial \tilde{\eta}^2} + \left(\alpha\tau\frac{\partial \bar{f}}{\partial \tilde{\eta}} - \frac{\partial \bar{g}}{\partial \tilde{\eta}}\right)\frac{\partial^2 \bar{g}}{\partial \tau \partial \tilde{\eta}} - \left(\alpha\tau\frac{\partial \bar{f}}{\partial \tau} - \frac{\partial \bar{g}}{\partial \tau}\right)\frac{\partial^2 \bar{g}}{\partial \tilde{\eta}^2} - (\alpha - 1)\frac{\partial \bar{f}}{\partial \tilde{\eta}}\frac{\partial \bar{g}}{\partial \tilde{\eta}} - (\alpha - 1)\left[\left(\frac{\partial \bar{f}}{\partial \tilde{\eta}}\right)^2 - U_0^2\right] = 0, \tag{3.10 b}$$

$$\bar{f} = \frac{\partial \bar{f}}{\partial \tilde{\eta}} = \bar{g} = \left.\frac{\partial \bar{g}}{\partial \tilde{\eta}}\right|_{\tilde{\eta}=0} = 0, \quad \left.\frac{\partial \bar{f}}{\partial \tilde{\eta}}\right|_{\tilde{\eta}=\infty} = U_0, \quad \left.\frac{\partial \bar{g}}{\partial \tilde{\eta}}\right|_{\tilde{\eta}=\infty} = 0. \tag{3.10 c}$$

Also,

$$\bar{v} = \frac{1}{2}\left(\tilde{\eta}\frac{\partial \bar{f}}{\partial \tilde{\eta}} - \bar{f}\right) + \alpha\tau\frac{\partial \bar{f}}{\partial \tau} - \frac{\partial \bar{g}}{\partial \tau}.$$

In the limit $\tau \to \infty$, system (3.10) must yield a Blasius solution for the function $\bar{f}$ and also lead to equation (3.6) for the crosswise velocity component, as required by matching with the solution at the main part of the plate. A comparison between (3.3) and (3.9) shows that

$$\tilde{f}(\tilde{\eta}, \varphi = 0) = \bar{f}(\tilde{\eta}, \tau = \infty) \quad \text{and} \quad w(\tilde{\eta}, \varphi = 0) = b\left[\frac{\partial \bar{f}}{\partial \tilde{\eta}} + \frac{\partial \bar{g}}{\partial \tilde{\eta}}\right](\tilde{\eta}, \tau = \infty).$$

Hence, functions $\bar{f}$ and $\bar{g}$ must satisfy the following equations:

$$\frac{\partial^3 \bar{f}}{\partial \tilde{\eta}^3} + \tfrac{1}{2}\bar{f}\frac{\partial^2 \bar{f}}{\partial \tilde{\eta}^2} = 0, \quad \bar{f} = \left.\frac{\partial \bar{f}}{\partial \tilde{\eta}}\right|_{\tilde{\eta}=0} = 0, \quad \left.\frac{\partial \bar{f}}{\partial \tilde{\eta}}\right|_{\tilde{\eta}=\infty} = U_0, \tag{3.11 a}$$

$$\frac{\partial^3 \bar{g}}{\partial \tilde{\eta}^3} + \tfrac{1}{2}\bar{f}\frac{\partial^2 \bar{g}}{\partial \tilde{\eta}^2} - (\alpha - 1)\left[\frac{\partial \bar{f}}{\partial \tilde{\eta}}\frac{\partial \bar{g}}{\partial \tilde{\eta}} + \left(\frac{\partial \bar{f}}{\partial \tilde{\eta}}\right)^2 - U_0^2\right] = 0, \quad \bar{g} = \left.\frac{\partial \bar{g}}{\partial \tilde{\eta}}\right|_{\tilde{\eta}=0} = \left.\frac{\partial \bar{g}}{\partial \tilde{\eta}}\right|_{\tilde{\eta}=\infty} = 0, \tag{3.11 b}$$

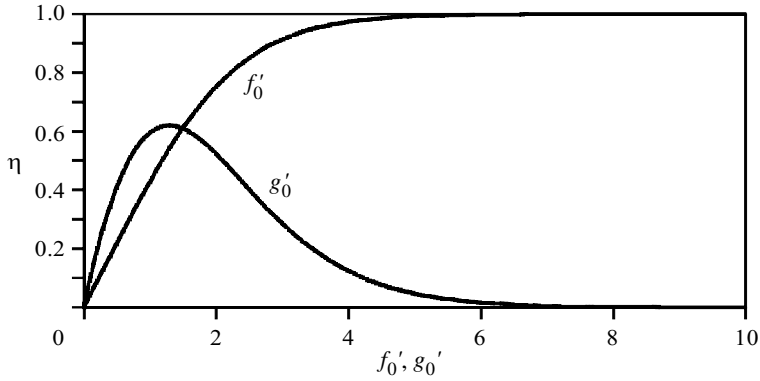

Figure 2. Numerical solutions for the functions $f_0'(\bar{\eta})$, $g_0'(\bar{\eta})$.

when τ tends to infinity. It may be observed that the solution to equations (3.11) also satisfies system (3.10). However, in this case the velocity component normal to the cusp surface does not vanish as τ tends to zero. Thus, in the vicinity of the cusp this solution should be discarded for the reasons presented in the previous section.

In order to shed some light on the flow structure near the rib of the corner formed by the cusp and the plate, consider the limit $\tau \to 0$, $\bar{\eta} = (\alpha-1)^{1/4}\tilde{\eta}/\tau^{1/4} = O(1)$. Then the solution to system (3.10) has the following form (as $\tau \to 0$):

$$\bar{f} = (\alpha-1)^{-1/4} f_0(\bar{\eta})\tau^{1/4} + \cdots, \qquad \bar{g} = (\alpha-1)^{1/4} g_0(\bar{\eta})\tau^{3/4} + \cdots. \tag{3.12}$$

The functions $f_0(\bar{\eta})$ and $g_0(\bar{\eta})$ satisfy the system:

$$f_0''' + \tfrac{3}{4} g_0 f_0'' = 0, \qquad g_0''' + \tfrac{3}{4} g_0 g_0'' - \tfrac{1}{2} g_0'^2 - f_0'^2 + U_0^2 = 0, \tag{3.13 a}$$

$$f_0(0) = f_0'(0) = 0, \qquad f_0'(\infty) = U_0, \qquad g_0(0) = g_0'(0) = 0, \qquad g_0'(\infty) = 0. \tag{3.13 b}$$

Here, primes stand for the derivatives with respect to $\bar{\eta}$. As expected, the velocity component normal to the cusp (i.e. $\partial\bar{g}/\partial\tilde{\eta}$) is now zero at $\tau = 0$. The functions $f_0'(\bar{\eta})$ and $g_0'(\bar{\eta})$ are plotted in figure 2 ($U_0 = 1$).

Limiting streamlines are given by the equation

$$z' = \left(c + \frac{\sqrt{b(\alpha-1)}}{\alpha} \frac{g_0''(0)}{f_0''(0)} (x')^{\alpha/2} \right)^2 + \frac{b(x')^\alpha}{\alpha} + \cdots, \tag{3.14}$$

$$f_0''(0) \approx 0.440, \quad g_0''(0) \approx 1.02,$$

where $c = \text{const}$. The case where $c > 0$ must be discarded, since it is contrary to the assumption of small τ made previously. When c is negative, limiting streamlines stem from the cusp in the outward direction. These limiting streamlines correspond to the boundary-layer flow that develops from the wall of the cusp towards the accessibility line (3.8). It is driven by the crosswise pressure gradient due to the cusp and is fully nonlinear.

An attempt to numerically integrate system (3.10) starting with the initial conditions (3.12) (say, using the Crank–Nicolson scheme) features numerical instability. It may be observed that numerical integration of system (3.10) with the initial conditions specified at $\tau = \infty$ in accordance with (3.11) also becomes unstable when τ is

PHILOSOPHICAL TRANSACTIONS OF THE ROYAL SOCIETY A MATHEMATICAL, PHYSICAL & ENGINEERING SCIENCES

small. The reason for this is that the coefficient $\alpha\tau\partial\bar{f}/\partial\tilde{\eta} - \partial\bar{g}/\partial\tilde{\eta}$ before the cross-stream derivatives of the velocity components $\partial/\partial\tau(\partial\bar{f}/\partial\tilde{\eta}, \partial\bar{g}/\partial\tilde{\eta})$ in system (3.10) changes its sign. The analysis of these numerical solutions shows that in the immediate vicinity of the section $\tau = 0$, this coefficient is negative for all $\tilde{\eta}$ (as is also apparent from (3.12)). This implies that the correct marching direction in this region is that of increasing τ. On the other hand, when τ is large, the above coefficient is positive, and the correct marching direction is that of decreasing τ. Between the sections $\tau = 0$ and $\tau = \infty$ there is a buffer domain where $\alpha\tau\partial\bar{f}/\partial\tilde{\eta} - \partial\bar{g}/\partial\tilde{\eta}$ is negative for small $\tilde{\eta}$ and positive for large $\tilde{\eta}$. Thus, whatever matching direction in τ is initially chosen, the resulting parabolic problem features inverse 'time' direction in this domain and is unstable to small perturbations of initial data (Lattes & Lions 1967). Unfortunately, owing to the instability, it is difficult to determine the boundaries of this domain reliably.

However, in the present context the change of marching direction is welcome, since it provides a scenario to simultaneously take into account the state of the flow both at $\tau = \infty$ and in the vicinity of the cusp surface $\tau = 0$. Indeed, in order to avoid the phenomenon of inverse 'time' direction for the parabolic system (3.10), we impose the initial conditions (3.12) as $\tau \to 0$ and (3.11) as $\tau \to \infty$, i.e. we seek the solution to the following problem:

$$\hat{u} = \frac{\partial\bar{f}}{\partial\tilde{\eta}}, \qquad \hat{w} = \frac{\partial\bar{g}}{\partial\tilde{\eta}}, \tag{3.15 a}$$

$$\frac{\partial^2\hat{u}}{\partial\tilde{\eta}^2} + \tfrac{1}{2}\bar{f}\frac{\partial\hat{u}}{\partial\tilde{\eta}} - (\hat{w} - \alpha\tau\hat{u})\frac{\partial\hat{u}}{\partial\tau} - \alpha\tau\frac{\partial\hat{u}}{\partial\tilde{\eta}}\frac{\partial\bar{f}}{\partial\tau} + \frac{\partial\hat{u}}{\partial\tilde{\eta}}\frac{\partial\bar{g}}{\partial\tau} = 0, \tag{3.15 b}$$

$$\frac{\partial^2\hat{w}}{\partial\tilde{\eta}^2} + \tfrac{1}{2}\bar{f}\frac{\partial\hat{w}}{\partial\tilde{\eta}} - (\hat{w} - \alpha\tau\hat{u})\frac{\partial\hat{w}}{\partial\tau} - \alpha\tau\frac{\partial\hat{w}}{\partial\tilde{\eta}}\frac{\partial\bar{f}}{\partial\tau} + \frac{\partial\hat{w}}{\partial\tilde{\eta}}\frac{\partial\bar{g}}{\partial\tau} - (\alpha - 1)(\hat{u}\hat{w} + \hat{u}^2 - U_0^2) = 0, \tag{3.15 c}$$

$$\hat{u} = \bar{f} = \hat{w} = \bar{g}|_{\tilde{\eta}=0} = 0, \quad \hat{u}(\tilde{\eta} \to \infty) = U_0, \quad \hat{w}(\tilde{\eta} \to \infty) = 0, \tag{3.15 d}$$

$$\hat{u}(\tau \to 0) = \frac{\partial f_0}{\partial\bar{\eta}}, \qquad \hat{w}(\tau \to 0) = \tau^{1/2}\frac{\partial g_0}{\partial\bar{\eta}}, \tag{3.15 e}$$

$$\hat{u}(\tau \to \infty) = \frac{\partial\bar{f}_\infty}{\partial\tilde{\eta}}, \qquad \hat{w}(\tau \to \infty) = \frac{\partial\bar{g}_\infty}{\partial\tilde{\eta}}. \tag{3.15 f}$$

Equations (3.15 *a*)–(3.15 *d*) are equivalent to (3.10), the initial conditions (3.15 *e*) follow from (3.12), the functions $\bar{f}_\infty(\tilde{\eta})$ and $\bar{g}_\infty(\tilde{\eta})$ satisfy systems (3.11 *a*) and (3.11 *b*), respectively.

The following note should be made in connection with the far-field boundary conditions (3.15 *f*). Recently, Dhanak & Duck (1997) showed that in certain situations the far-field conditions may permit several branches of solution and, thus, be a potential source of non-uniqueness. However, since equation (3.11 *b*) is linear, this is not the case with problem (3.15). It may be shown that the solution to system (3.11 *a*), (3.11 *b*), which in effect determines the functions on the right-hand sides of (3.15 *f*), is unique for all $\alpha > 1$.

In order to construct a numerical solution to system (3.15), we adopt the approach similar to that proposed by Korolev for triple-deck interactions (Sychev *et al.* 1987, pp. 238–244). However, in the present context we do not make an allowance for

viscous–inviscid interaction, since there is no *a priori* evidence that the solution to system (3.15) may feature any singularity.

Let $a = \bar{f}(\tilde{\eta})/2$, $c = \hat{w} - \alpha\tau\hat{u}$,

$$V = \begin{pmatrix} \hat{u} \\ \hat{w} \end{pmatrix}, \qquad B = -(\alpha - 1)\begin{pmatrix} 0 \\ \hat{u}\hat{w} + \hat{u}^2 - U_0^2 \end{pmatrix}, \qquad D = \alpha\tau\frac{\partial V}{\partial \tilde{\eta}}, \qquad E = -\frac{\partial V}{\partial \tilde{\eta}},$$

$$V^* = \frac{\partial}{\partial \bar{\eta}}\begin{pmatrix} f_0(\bar{\eta}) \\ \tau^{1/2} g_0(\bar{\eta}) \end{pmatrix}, \qquad V^{**} = \frac{\mathrm{d}}{\mathrm{d}\tilde{\eta}}\begin{pmatrix} \bar{f}_\infty(\tilde{\eta}) \\ \bar{g}_\infty(\tilde{\eta}) \end{pmatrix}, \qquad V^\infty = \begin{pmatrix} U_0 \\ 0 \end{pmatrix}.$$

Problem (3.15) can then be rewritten as follows:

$$\frac{\partial^2 V}{\partial \tilde{\eta}^2} + a\frac{\partial V}{\partial \tilde{\eta}} - c\frac{\partial V}{\partial \tau} - D\frac{\partial \bar{f}}{\partial \tau} - E\frac{\partial \bar{g}}{\partial \tau} + B = 0, \tag{3.16 a}$$

$$V = \frac{\partial}{\partial \tilde{\eta}}\begin{pmatrix} \bar{f} \\ \bar{g} \end{pmatrix}, \tag{3.16 b}$$

$$V|_{\tilde{\eta}=0} = 0, \qquad V|_{\tilde{\eta}=\infty} = V^\infty, \qquad V|_{\tau\to 0} = V^*, \qquad V|_{\tau=\infty} = V^{**}. \tag{3.16 c}$$

Consider the following finite-difference approximations of equations (3.16 *a*) and (3.16 *b*):

$$\frac{V_{jk+1} - 2V_{jk} + V_{jk-1}}{(\Delta\eta)^2} + a_{j,k}\frac{V_{j,k+1} - V_{j,k-1}}{2\Delta\eta} - |c_{j,k}|\frac{V_{j,k} - V_{j-s,k}}{\Delta\tau}$$
$$- D_{j,k}\frac{\bar{f}_{j,k} - \bar{f}_{j-1,k}}{\Delta\tau} - E_{j,k}\frac{\bar{g}_{j,k} - \bar{g}_{j-1,k}}{\Delta\tau} + B_{j,k} = 0,$$
$$j = 1, 2, \ldots, M-1, \quad k = 1, 2, \ldots, N-1, \tag{3.17 a}$$

$$\bar{f}_{j,k} = \bar{f}_{j,0} + \Delta\eta\sum_{i=1}^{k}\tfrac{1}{2}(\hat{u}_{j,i} + \hat{u}_{j,i-1}), \quad \bar{g}_{j,k} = \bar{g}_{j,0} + \Delta\eta\sum_{i=1}^{k}\tfrac{1}{2}(\hat{w}_{j,i} + \hat{w}_{j,i-1}),$$
$$j = 1, 2, \ldots, M, \quad k = 1, 2, \ldots, N, \tag{3.17 b}$$

which are second-order accurate in $\tilde{\eta}$ and first-order accurate in τ. Here, $F(\tau = \tau_j, \tilde{\eta} = \tilde{\eta}_k) = F_{j,k}$ for any function $F(\tau, \tilde{\eta})$, $\tau_j = \varepsilon + j\Delta\tau$, $j = 0, 1, \ldots, M$, and $\tilde{\eta}_k = k\Delta\eta$, $k = 0, 1, \ldots, N$. M and N are some large integers, $\varepsilon > 0$ is a sufficiently small number. Also, $s = \mathrm{sing}(c_{j,k})$, i.e.

$$\frac{\partial V}{\partial \tau} \approx (V_{j,k} - V_{j-1,k})/\Delta\tau, \quad \text{for } c_{j,k} \geqslant 0$$

and

$$\frac{\partial V}{\partial \tau} \approx (V_{j+1,k} - V_{j,k})/\Delta\tau, \quad \text{for } c_{j,k} < 0.$$

The no-slip and outer conditions become

$$V_{j,0} = \bar{f}_{j,0} = \bar{g}_{j,0} = 0, \quad V_{j,N} = V^\infty, \quad j = 1, 2, \ldots, M-1. \tag{3.17 c}$$

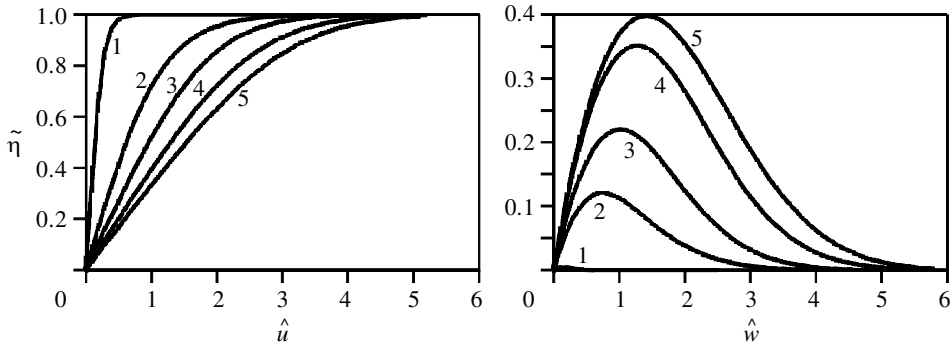

Figure 3. Longitudinal and crosswise velocity profiles in the inner region: 1, $\tau = 0.0001$; 2, $\tau = 0.2$; 3, $\tau = 0.6$; 4, $\tau = 5.0$; 5, $\tau = 10.0$.

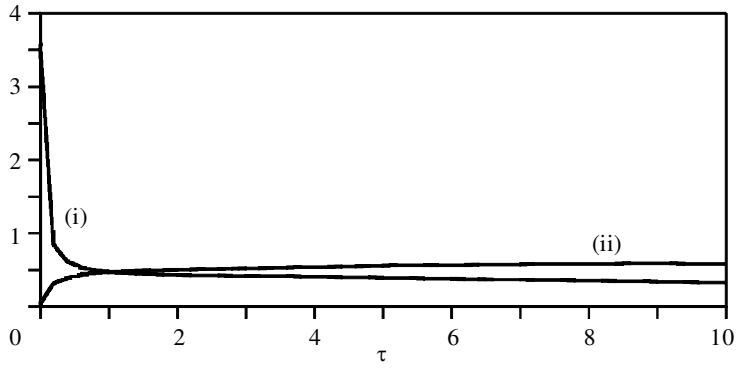

Figure 4. Distribution of the skin friction coefficients in the inner region: (i) $\partial\tilde{u}/\partial\tilde{\eta}(\tilde{\eta}=0)$; (ii) $\partial\tilde{w}/\partial\tilde{\eta}(\tilde{\eta}=0)$.

The conditions in τ are approximated as follows:

$$V_{0,k} = V_{0,k}^{*}, \quad V_{M,k} = V_{k}^{**}, \quad k = 0, 1, \ldots, N. \tag{3.17 d}$$

Since system (3.17) is nonlinear—and, as we have already seen, there is no marching direction for it—global iterations are needed in order to obtain the solution. The simplest approach is to solve system (3.17) for $V_{j,k}$ assuming that the coefficients $a_{j,k}$, $B_{j,k}$, $c_{j,k}$, $D_{j,k}$, $E_{j,k}$ are known from the previous iteration. This can be done, say, with the help of the generalized Thomas algorithm (see Fletcher 1991, pp. 238–246). Then the above coefficients can be calculated again and the iteration cycle repeated.

The calculations were carried out with $M = 50$, $N = 80$, $\Delta\tau = 0.2$, $\Delta\eta = 0.1$, with the values of the outer boundaries being $\tau_\infty = M\Delta\tau = 10$ and $\tilde{\eta}_\infty = N\Delta\eta = 8$. In order to test the accuracy of the scheme, the calculations were repeated with the maximum values of $\Delta\tau$ and $\Delta\eta$ being lowered by a factor of three and two, respectively. The maximum values of the outer boundaries were increased by a factor of 1.5. The iterations were terminated when the maximum difference between the two subsequent approximations of the solution was less that 10^{-6}. It usually took about 23 iterations to achieve this level of convergence. Variations of the obtained solutions were within 1%. Typical velocity and skin friction patterns are presented in figures 3 and 4 ($\alpha = 1.5$, $U_0 = b = 1$).

4. Discussion

This study has concentrated on the structure of the boundary-layer flow developing at a flat plate under the action of the pressure gradient caused by a cusp secured to the plate's surface. The major findings of the work are as follows.

The plate's boundary-layer flow near the curvilinear corner formed by the cusp and the plate consists of two characteristic domains: an outer region (i.e. the main part of the boundary layer considered in § 3 *a*), and an inner region in the immediate vicinity of the rib of the corner (i.e. the nonlinear sublayer near the cusp wall, see § 3 *b*). The outer boundary-layer flow starts at the leading edge of the plate and occupies most of its surface. The flow is quasi-two-dimensional here, with the cross-stream momentum equation being linear. Since the velocity component orthogonal to the cusp does not vanish at its surface, this flow is separated from the wall of the corner by an accessibility line (3.8) and never reaches it.

The inner region lies near the cusp surface and contains another boundary-layer flow. The latter originates at the wall of the cusp and is driven by the crosswise pressure gradient outward. It has the same vertical thickness as the outer region, but the growth of the cross-stream perturbations near the cusp makes it fully nonlinear. The inner region is characterized by the existence of a buffer zone where the inner flow meets with the outer boundary layer, which develops from the leading edge of the plate. The most striking feature of the inner region is that, though its governing equations are inherently parabolic, two initial conditions are needed to determine the solution uniquely. One of them must be stated at the cusp surface and the other one at the interface of the inner and the outer regions. This is possible only thanks to the change of sign of the coefficient before the crosswise derivative of the velocity in the governing equations, which controls the direction of disturbance propagation. It is this anomalous behaviour of the governing equations in the buffer region that provides a mechanism for the two boundary-layer flows above to merge smoothly.

In conclusion, we should like to consider the obtained results in the context of the previous work, and especially that of Rubin (1966), which describes the limiting case of a 90° streamwise corner formed by two flat plates.

It should be noted that the emergence of the double structure discovered above is entirely due to the curvature of the cusp $\kappa \approx -b(\alpha-1)(x')^{\alpha-2}+\cdots$, $x' \to 0$. If the curvature were to be identically zero (i.e. $b=0$), the double structure would vanish and we would arrive at the classical Blasius solution for the whole of the plate. This would be exactly the result obtained by Rubin (1966) for region II of his paper. Thus, we see that the curvature of the wall radically changes the structure of the plate's boundary layer near the rib of the corner. It may be shown that while the flow in the boundary layer that develops along the cusp wall (region III in Rubin's notation) remains almost unaffected by the curvature, the structure of the overlap region (termed the 'corner layer' in Rubin (1966)) becomes somewhat different. Since the main objective of this work is to examine possible changes in the plate's boundary layer provoked by the curvature of the wall, rather than the effects confined to the corner layer, and owing to the restrictions imposed on the size of the paper, we shall take only a brief look at the features of the corner layer here.

Consider first the boundary-layer flow which develops over the cusp surface in the vicinity of its leading edge. Its thickness is $O(Re^{-1/2})$, and the appropriate boundary-layer coordinate is $\zeta \sim nRe^{1/2}$. Here n is the normal distance to the cusp.

At a sufficiently small vertical distance y' from the plate, this boundary-layer flow overlaps with the boundary-layer flow over the plate.

On the other hand, we have seen in § 3 *b* that solution (3.12), which describes the boundary-layer flow over the plate in the immediate vicinity of the cusp wall, is characterized by the local vertical variable $\bar{\eta}$. Since, in the vicinity of the origin, $n \approx z' - b(x')^{\alpha}/\alpha$, we find that $\bar{\eta} \approx (-\kappa)^{1/4} Re^{1/2} y'/n^{1/4}$. By virtue of the fact that the characteristic length-scales ζ and $\bar{\eta}$ must be of equal order of magnitude in the overlap region, we obtain the following asymptotic relationship

$$y' \sim n^{5/4}/(-\kappa)^{1/4}. \tag{4.1}$$

If we now assume that $n = O(Re^{-1/2})$, then the correct vertical scaling for the overlap region in the present flow situation appears to be $O(Re^{-5/8})$, rather than $O(Re^{-1/2})$ as is the case with the corner with flat walls. The case of a 90° streamwise corner formed by two flat plates is recovered when the curvature of the cusp, κ, becomes sufficiently small. Indeed, if we assume that $b = O(Re^{-1/2})$, then y' becomes $O(Re^{-1/2})$ in the overlap region, as suggested by expression (4.1).

It may be inferred from the above discussion that the vertical extent of the overlap region must depend on the order of magnitude of the curvature of the wall. A more detailed quantitative analysis of the flow structure in the overlap region is obviously needed. This study is currently under way.

The author thanks the referees for their useful comments and suggestions.

References

Abramovitz, M. & Stegun, I. 1979 *Handbook on mathematical functions*. Moscow: Nauka. (Russian edition.)

Anderson, D. A., Tannehill, J. C. & Pletcher, R. H. 1990 *Computational fluid mechanics and heat transfer*, vol. 2, ch. 8, § 8.6. Moscow: MIR. (Russian edition.)

Dhanak, M. R. & Duck, P. W. 1997 The effects of freestream pressure gradient on a corner boundary layer. *Proc. R. Soc. Lond.* A **453**, 1793–1815

Fletcher, C. A. J. 1991 *Computational techniques for fluid dynamics*, vol. 1: *Fundamental and general techniques*. Springer. (Russian edition.)

Imai, I. 1953 Discontinuous potential flow as the limiting form of the viscous flow for vanishing viscosity. *J. Phys. Soc. Japan* **8**, 399.

Lattes, R. & Lions, J.-L. 1967 *Méthode de quasi-reversibilité et applications*. Paris: Dunod.

Nazarov, S. A. & Plamenevskij, B. A. 1991 Elliptic problems in domains with piecewise smooth boundaries. Moscow: Nauka. (In Russian.)

Rubin, S. G. 1966 Incompressible flow along a corner. *J. Fluid Mech.* **26**, 97–110.

Smith, F. T. & Gajjar, J. 1984 Flow past wing–body junctions. *J. Fluid Mech.* **144**, 191–215.

Sychev, V. V., Ruban, A. I., Sychev, Vic. V. & Korolev, G. L. 1987 *Asymptotic theory of separating flows* (ed. V. V. Sychev). Moscow: Nauka. (In Russian.)

Walton, A. G. & Smith, F. T. 1997 Concerning three-dimensional flow past a tall building on flat ground. *Q. J. Appl. Math.* **50**, 97–128.